Macromolecules

Article

pubs.acs.org/Macromolecules

Mechanism of Isotactic Styrene Polymerization with a C_6F_5-Substituted Bis(phenoxyimine) Titanium System

Lucia Caporaso,[†,*] Marianna Loria,[†] Mina Mazzeo,[†] Kenji Michiue,[‡] Takashi Nakano,[§] Terunori Fujita,[⊥,*] and Luigi Cavallo[∥]

[†]Department of Chemistry and Biology, University of Salerno, Via Ponte Don Melillo, 84084 Fisciano, Salerno, Italy

[‡]Catalysis Science Laboratory, Research Center, Mitsui Chemicals, Inc., 580-32 Nagaura, Sodegaura-City Chiba 299-0265, Japan

[§]Material Science Laboratory, Research Center, Mitsui Chemicals, Inc., 580-32 Nagaura, Sodegaura-City Chiba 299-0265, Japan

[⊥]Mitsui Chemicals Singapore R&D Center Pte. Ltd., 50 Science Park Road, #06-08 The Kendall, Singapore Science Park II Singapore 117406

[∥]King Abdullah University of Science and Technology, Physical Sciences and Engineering, Kaust Catalysis Center, Thuwal 23955-6900, Saudi Arabia

Supporting Information

ABSTRACT: We report a combined, experimental and theoretical, study of styrene polymerization to clarify the regio- and stereocontrol mechanism operating with a C_6F_5-substituted bis(phenoxyimine) titanium dichloride complex. Styrene homopolymerization, styrene−propene and styrene−ethene−propene copolymerizations have been carried out to this aim. A combination of ^{13}C NMR analysis of the chain-end groups and of the microstructure of the homopolymers and copolymers reveals that styrene polymerization is highly regioselective and occurs prevalently through 2,1-monomer insertion. DFT calculations evidenced that steric interaction between the growing chain and the monomer in the transition state insertion stage is at the origin of this selectivity. The formation of isotactic polystyrene with a chain-end like microstructure is rationalized on the base of a mechanism similar to that proposed for the syndiospecific propene polymerization catalyzed by bis(phenoxyimine) titanium dichloride complexes. Finally, a general stereocontrol mechanism operative in olefin polymerization with this class of complexes is proposed.

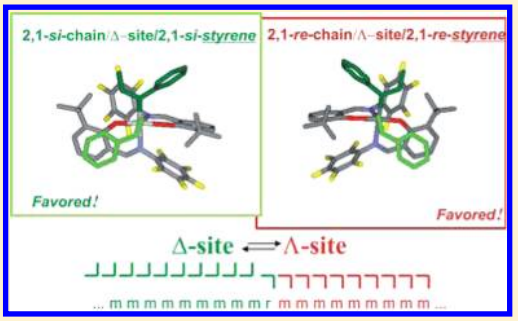

INTRODUCTION

The advancement of molecular olefin polymerization catalysis, as represented by the development of group 4 metallocene[1] and postmetallocene[2] catalysts, has given scientists greater insight into polymerization mechanisms.[3] Within this large amount of work, phenoxy-imine ligated early transition metal complexes (aka FI catalysts) for the oligomerization[4] and polymerization of olefinic monomers,[5] developed by researchers at Mitsui Chemicals, have achieved a quite remarkable role as model systems with peculiar polymerization behavior, as well as systems with potential industrial application. To date, FI catalysts demonstrate unprecedentedly high ethene insertion efficiency (maximum turnover frequency, TOF 3.9×10^6 h^{-1}), which represents the highest catalytic activity and productivity for molecular catalysis.[5g] Additionally, FI catalysts display unique catalytic properties that include precise control over chain transfer reactions (including living polymerization),[6−8] extremely high ethene selectivity to α-olefins,[9] very high reactivity toward cyclic olefins,[10] high functional group tolerance,[11] highly isoselective enchainments of both propene[12] and styrene monomers,[13] highly syndioselective propene polymerization despite a C_2 symmetric nature,[14] and MAO- and borate-free polymerization ($MgCl_2$ cocatalyst system).[15]

Of these, highly isoselective styrene polymerization with C_6F_5-substituted bis(phenoxyimine) titanium dichloride complexes having a nonbridged and fluxional character represents one of the most intriguing catalytic properties since molecular catalysts for isotactic polystyrene (iPS) usually possess a bridged and rigid ligand framework.[16] In this article, we discuss the mechanisms for isoselective styrene polymerization with bis[*N*-(3-*tert*-butylsalicylidene)-2,3,4,5,6-pentafluoroanilinato]-titanium(IV) dichloride complex, (**Ti−FI**) (see Scheme 1) by a combined experimental and theoretical approach. Experimentally, we tackled this study with two different goals in mind. The first is to clarify the regiochemistry of monomer insertion and the mechanism of stereocontrol operative for isotactic styrene polymerization promoted by the bis[*N*-(3-*tert*-butylsalicylidene)-2,3,4,5,6-pentafluoroanilinato]titanium(IV) dichloride complex, performing a detailed ^{13}C NMR analysis of the chain-end groups and of the microstructure of the homopolymers obtained under the same conditions reported in a previous paper.[13] The latter goal of this work is to study the

Received: August 2, 2012
Revised: October 2, 2012
Published: October 19, 2012

Scheme 1

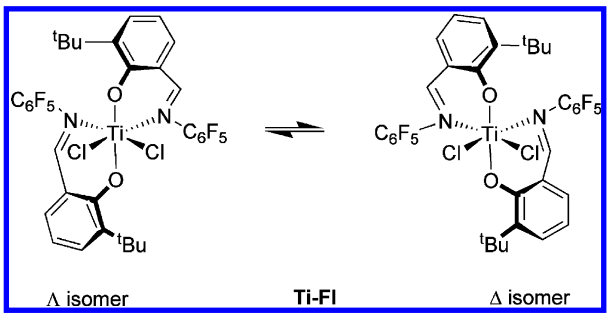

microstructure of styrene−propene [P(S−P)] copolymers and styrene−ethene−propene [P(S−E/P)] copolymers obtained with a low amount of ethene in the feed. This allowed to establish the regiochemistry of styrene insertion and to compare it to that of propene insertion (P−S copolymers) with **Ti−FI** based systems, and to study the effect of the Cα and Cβ substitution in Ti-chain propagating species on the styrene insertion mode during chain growth. Theoretically, the mechanism of regio- and stereocontrol operative in styrene polymerization with **Ti−FI** based systems was rationalized by DFT calculations. The transition states (TS) for styrene insertion into the Ti−Me, Ti−Et, Ti−^{i}Pr and Ti−^{i}Bu bonds were located to rationalize styrene selectivities in the first insertion step, in the styrene−propene and styrene−ethene−propene copolymerizations. The experimental regio- and stereochemistry of the styrene insertion during the propagation steps were explained by comparing the competitive TSs with both 1,2- and 2,1-styrene ending chains.

RESULTS AND DISCUSSION

1. Styrene Homopolymerization. We performed styrene polymerizations under the same reaction conditions reported in the previous paper.[13] All the obtained polymers were first purified from atactic PS fractions by extraction in methyl ethyl ketone (MEK). The MEK-insoluble fractions (>99%) were analyzed by ^{1}H NMR spectroscopy. Since in all cases mixtures of isotactic and syndiotactic polystyrenes (iPS and sPS in the following) were obtained, we separated them by extraction in $CHCl_3$ at room temperature. The isotactic $CHCl_3$-soluble fractions (iPS) were analyzed by GPC analyses and by ^{13}C NMR spectroscopy. The polymerization results and the polymers characterization data are reported in Table 1.

The results reported in Table 1 indicate that the catalyst behavior depends on the polymerization temperature, on the Al/Ti ratio and on the reaction time. By increasing the Al/Ti ratio and the reaction time, the iPS/sPS ratio decreases since both parameters favor the reduction of the oxidation state of the titanium from IV to III, and it is well-known that Ti(III) species are particularly active in the synthesis of sPS[17] (compare run 1 with run 3 and run 3 with run 4 of Table1). Focusing on temperature, only traces of polymers were obtained in 16 h if the polymerization temperature is decreased from 25 to 0 °C, (compare run 2 with runs 3 and 4). Increasing the temperature up to 50 °C results in a decrease of the iPS/sPS ratio (compare run 4 with run 5), indicating that higher temperature facilitates reduction of Ti(IV) to Ti(III). The ^{13}C NMR spectrum of the $CHCl_3$-soluble fraction of polystyrene obtained at 25 °C in the presence of the catalytic system **Ti−FI**/DMAO (run 4; Table1) is displayed in Figure 1.

Table 1. Styrene Polymerizations with Ti−FI/ DMAO[a]

run	Al/Ti	T (°C)	t (h)	iPS/sPS[b]	yield (mg)[c]	M_w/M_n[d]	M_n (×10^3)[d]
1	250	25	1	–	traces	–	–
2	200	0	16	–	traces	–	–
3	200	25	3	80/20	20	–	–
4	200	25	6	47/53	265	1.5	5.1
5	200	50	6	1/99	300	1.3	3.0

[a]Conditions: toluene 30 mL, styrene 100 mL, and [Ti] = 2 × 10^{-3} M; MEK-soluble fractions <1%. [b]Determined by ^{1}H NMR. [c]Yield of iPS ($CHCl_3$-soluble fraction). [d]Determined by GPC.

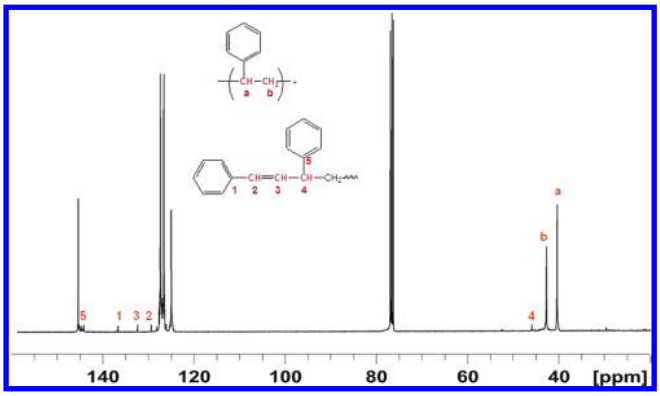

Figure 1. ^{13}C NMR spectrum (100 MHz, $CDCl_3$, 298 K) of the $CHCl_3$-soluble fraction of polystyrene (run 4, Table 1). The chemical shifts are in ppm downfield of HMDS.

The acquisition time of the ^{13}C NMR spectrum of Figure 1 is 4 days. This long acquisition time allowed us to detect the resonances relative to the chain-end groups and to the stereoerrors which were below the NMR detection level in the ^{13}C NMR spectrum previously reported.[13] The more detailed ^{13}C NMR spectrum reveals main resonances diagnostic of the iPS monomer units (*e.g.*, **a** and **b** in Figure 1), and additional less intense resonances attributable, according to the literature,[16d,18] to unsaturated chain-end groups such as *trans* 1,3-diphenyl-1-butenyl group (Figure S1 of Supporting Information). These end groups are consistent with chain termination occurring via β −H elimination from a 2,1-styrene unit (1−5 signals in Figure 1). The resonances diagnostic of unsaturated chain end group arising from β −H elimination from a 1,2-styrene unit were not detected.[16d,18] The strict agreement between the M_n values measured by GPC analyses and the M_n values calculated by NMR spectroscopy (values obtained from the resonance area of methine carbon −**C**H−Ph in the unsaturated chain end groups, and of the methine carbon (−**C**H(Ph)− in the chain) suggested that the β −H elimination (to the metal or to the monomer) of the chain should be the main termination reaction. Conversely, the first insertion step, corresponding to styrene insertion into the Ti−Me and Ti−H bonds, is not regiospecific, since the saturated chain-end groups arising from both 1,2- and 2,1-styrene insertion were detected.

The vertically expanded aliphatic region of the spectrum, from 11 to 36 ppm, is reported in Figure 2. On the basis of literature,[16b,18,19] the signals 1*t* and 1*e* were attributed to the methyl carbons of the *threo* and *erythro* stereiosomers formed after two subsequent 2,1-styrene insertions into the Ti−H bond, whereas signals 5 and 6 were attributed to the methylene carbons of the sequences formed from two successive 1,2-

dx.doi.org/10.1021/ma301631b | *Macromolecules* 2012, 45, 8588−8597

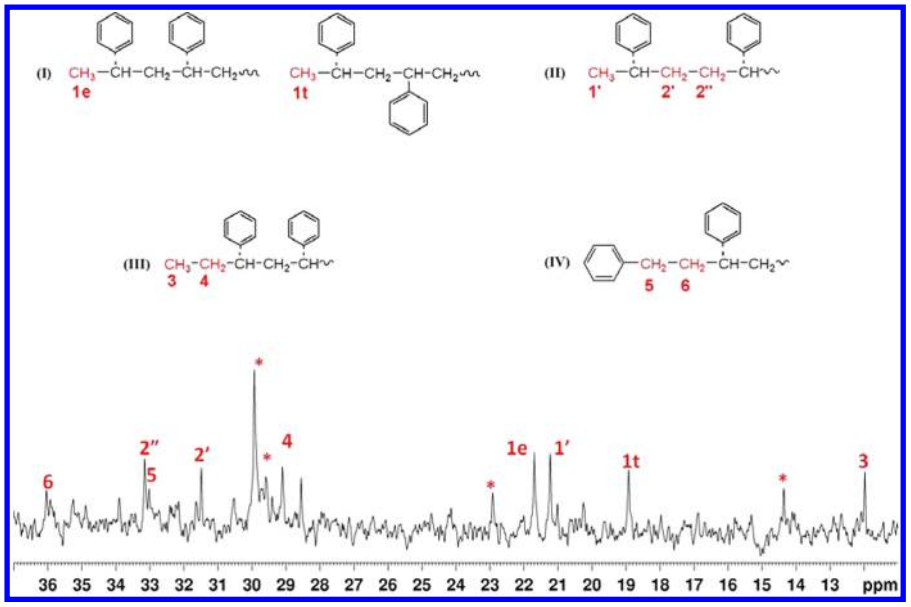

Figure 2. Vertically expanded aliphatic region of the spectrum reported in Figure 1 (run 4 of Table 1). The asterisk indicates the ethene sequences resonances due to traces of $Al(Me)_3$ in the reaction system.[19]

styrene insertions into the same Ti−H bond. Additional weak resonances relative to saturated end groups formed in the initiation steps by styrene insertion into the Ti−Me bond, both with 1,2- and 2,1-regiochemistry, were observed. Specifically, signals 3 and 4 were attributed to the sequence arising from two subsequent 2,1-styrene insertions into the Ti−Me bond. Finally, signals 1′ and 2′ were attributed to the sequence arising from 1,2-styrene insertion into the Ti−Me bond followed by a subsequent styrene insertion that occurs with opposite regiochemistry (2,1-styrene insertion).

These results suggest that the regioselectivity of styrene insertion in the isotactic polymerization catalyzed by the **Ti−FI**/DMAO system is prevailingly 2,1. Conversely, a low regioselectivity is observed in the initiation steps, since both 2,1- and 1,2-styrene insertions are possible into the Ti−H and Ti−Me bonds.

To clarify the mechanism of stereocontrol operating in the styrene polymerization with the **Ti−FI**/DMAO system, a thorough characterization of the quaternary aromatic carbon resonances of a ^{13}C NMR spectrum at heptad level was performed (see Figure 3). The presence of a sharp resonance at 146.50 ppm, assigned to the aromatic *ipso* carbon in a *mmmmmm* heptad indicates the highly isotactic microstructure of the sample [*mmmmmm*] = 96%. On the basis of recent literature data,[20−22] the three additional less intense resonances at 146.32, 146.17, and 145.74 ppm, of equal intensities, were assigned to the *mmmmmr*, *mmmmrm* and *mmmrmm* heptads, respectively. This finding suggests that the mechanism of stereocontrol operating in the isotactic styrene polymerization with the **FI−Ti**/DMAO catalytic system is chain end-like.

2. Styrene Copolymerizations. *a. Styrene−Propene Copolymers P(S−P).* Styrene−propene polymerizations were carried out under various reaction conditions.[23] The polymers were extracted with MEK and the insoluble fractions were analyzed by GPC and ^{13}C NMR techniques. The polymerization conditions and the characterization results are summarized in Table 2.

The results reported in Table 2 show that by decreasing the [P]/[S] ratio in the feed, the amount of the styrene units in the

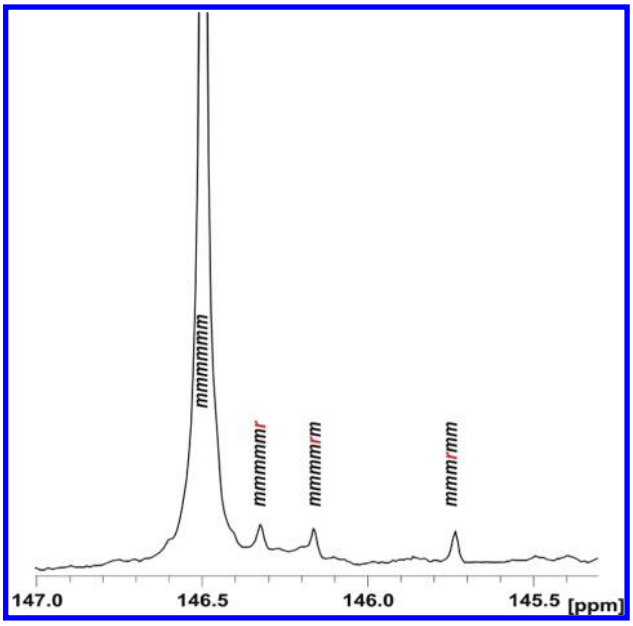

Figure 3. Vertically expanded quaternary aromatic carbon region of a ^{13}C NMR spectrum of the sample obtained in run 4 of Table 1 (100 MHz, $CDCl_3$, 298 K).

Table 2. Styrene−Propene Copolymerizations with Ti−FI/DMAO[a] and Copolymers Composition

run	Al/Ti	mmol of Ti	[P]/[S][b]	*t* (h)	yield (mg)[c]	M_w/M_n[c,d]	%S[c,e]
1	100	0.1	0.3	16	2000	1.38	0.5
2	100	0.1	0.1	16	100	1.29	5.0
3	200	0.3	0.1	16	80	1.25	5.2
4	100	0.1	0.05	16	traces	n.d.	n.d.
5	200	0.3	0.05	6	120	1.65	10.0

[a]Conditions: toluene 30 mL, styrene 100 mL, and T = 25 °C. [b]Mole ratio of propene and styrene in the feed. [c]Results relative to MEK-insoluble polymer fractions (>99%). [d]Determined by GPC. [e]Styrene content determined by ^{13}C NMR.

dx.doi.org/10.1021/ma301631b | *Macromolecules* 2012, 45, 8588−8597

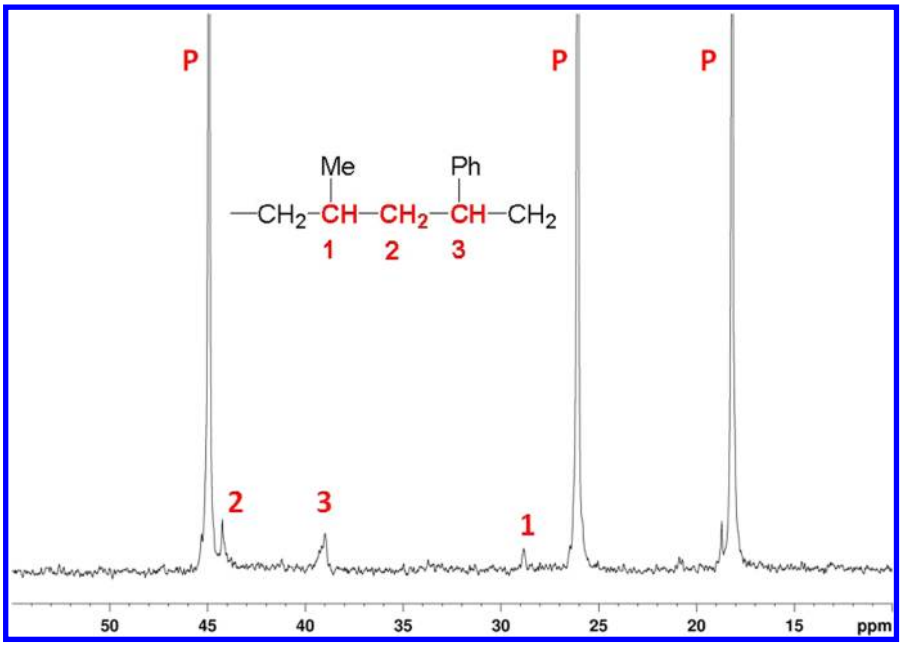

Figure 4. Aliphatic region of ^{13}C NMR spectrum (75 MHz, TCDE, 393 K) of the P(S−P) copolymer of run 3 of Table 2. The chemical shifts are in ppm downfield from HMDS.

Scheme 2

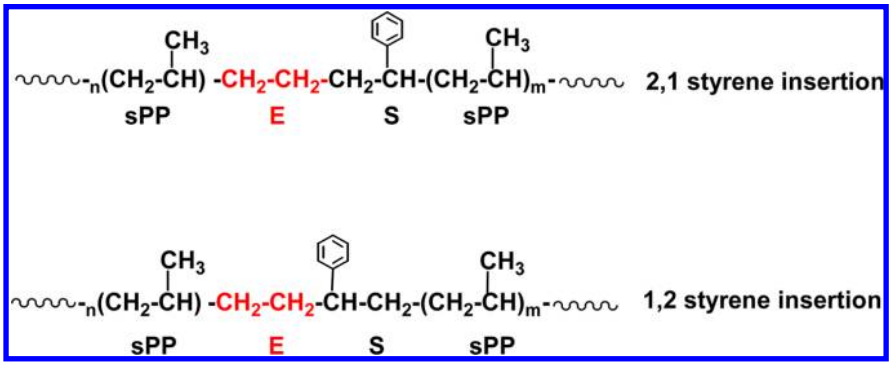

copolymers increases but, at the same time, the catalytic activity decreases (compare, *e.g.*, run 1 with run 2, Table 2). By comparing run 2 with run 3 we can observe that, at the same [P]/[S] ratio and polymerization time, the yield of run 3 is lower than that of run 2, despite the higher [Ti] in the feed, because of the high Al/Ti ratio. The reason seems the reduction of the Ti(IV) active species to Ti(III) species that are not able to copolymerize styrene with propene.[24] As an example, in Figure 4, the aliphatic region of the ^{13}C NMR spectrum of the run 3 of Table 2 is reported with the signals attributions.

The ^{13}CNMR analysis reveals that all the copolymers are characterized by syndiotactic propene sequences joined by isolated styrene units. As a matter of fact, in the spectrum of Figure 4, in addition to the peaks of the syndiotactic polypropene (signal P), three new resonances emerge (1, 2, and 3 of the sequence reported in Figure 4), which we attributed to isolated styrene units joined to propene sequences.[21,24,25] Interestingly, these additional resonances reveal that adjacent styrene−propene units show the same regiochemistry of insertion. Since the 2,1-propene insertion is strongly supported by several experimental evidences and theoretical calculations for the **Ti−FI** based systems,[3a,6b,14f,26,27] the observed microstructure suggests a prevalent 2,1-styrene insertion, accordingly the evidence concerning the styrene polymerization results already discussed in the previous paragraph.

b. Styrene−Ethene−Propene Copolymers P(S−E/P). The styrene−ethene−propene copolymers have been prepared with the **Ti−FI** catalyst following the synthetic procedure described for the synthesis of isotactic polypropylene containing isolated ethene/styrene units by using *ansa*-zirconocene based catalysts.[24,25]

The most active monomer, ethene, can easily insert in the growing chain after insertion of both styrene and propene, reactivating chain growth. As a consequence, by using an opportune small amount of ethene and an appropriated [P]/[S] ratio in the feed, sequences formed from consecutive propene−ethene−styrene insertions could be obtained. On the basis of the relative regiochemistry of styrene and propene insertions, two different sequences of the three monomers in the chain should be observed, as reported in Scheme 2. This synthetic strategy provides useful information about the styrene insertion mode, relative to the propene, after the ethene insertion.

dx.doi.org/10.1021/ma301631b | *Macromolecules* 2012, 45, 8588−8597

All copolymerizations have been performed by bubbling at 0.2 L/min a gaseous mixture of propene and ethene, of opportune composition, at atmospheric pressure into a flask containing a styrene solution of the **Ti−FI** /DMAO system. The obtained copolymers were extracted with MEK and the insoluble fractions were analyzed by GPC and ^{13}C NMR techniques. The GPC analyses showed that all copolymers have monomodal molecular weight distribution characterized by narrow polydispersity indexes $M_w/M_n \leq 2$. The reaction conditions and the main characterization data are reported in Table 3. The aliphatic region of ^{13}C NMR spectrum copolymer obtained in run 3 has been reported as example in Figure 5.

Table 3. Styrene−Ethene−Propene Copolymerizations with Ti−FI/DMAO[a] and Copolymer Composition

run	Ti (mmol)	[E]/[P]/[S][b]	t (h)	yield[c] (mg)	% E[d]	% P[d]	% S[d]
1	0.1	[1]/[25]/[430]	1	100	91.2	8.1	0.7
2	0.1	[1]/[58]/[587]	3	85	75.3	23.6	1.1
3	0.2	[1]/[300]/[2900]	6	45	2.3	96.0	1.7

[a]Conditions: toluene 30 mL, styrene 100 mL, and T = 25 °C. [b]Mole ratio of ethene, propene and styrene in the feed. [c]Results are based on MEK-insoluble polymers. [d]Copolymer composition determined by ^{13}C NMR.

The ^{13}C NMR analysis revels that the copolymers are substantially composed by syndiotactic polypropylene sequences (signals P) joined to the following: (i) isolated ethene unit (signals f, g, and h, Figure 5), (ii) consecutive ethene−styrene units originated for 2,1-styrene insertions (signals i and j, Figure 5); (iii) consecutive ethene−styrene units originated for 1,2-styrene insertions (signals a, b, c, d, and e, Figure 5).[24,25] As a consequence, both 1,2- and 2,1-styrene insertions occur after an ethene insertion. However, by comparing the intensity of the peaks corresponding to the two sequences (*e.g.*, compare the signal j with signal b of Figure 5), the 1,2-styrene insertion seems to prevail on the competitive styrene insertion into Ti−CH_2−CH_2−P_n bond.

In conclusion, the results herein reported on the styrene homopolymerization and copolymerizations catalyzed by the **Ti−FI**/DMAO system clearly demonstrated: (a) the polystyrene is isotactic with a microstructure compatible with a chain end like stereocontrol mechanism; (b) the styrene homopolymerization is highly regioselective and occurs prevalently with 2,1-styrene insertion mode; (c) the styrene insertion into the Ti−Me bond can occur with both 1,2- and 2,1-modes, but the following styrene insertion takes place prevalently in 2,1-mode in all cases; (d) styrene and propene insert with the same regiochemistry (2,1-mode); (e) both 1,2- and 2,1-styrene insertion modes take place on the Ti−CH_2−CH_2−P_n bond.

These findings suggest that steric interaction between the styrene monomer and the Cα and Cβ substituents of the chain favors the 2,1-styrene insertion mode during the propagation steps.

■ COMPUTATIONAL RESULTS

Density functional theory calculations were performed to rationalize from a mechanistic perspective the experimental results. We started by considering the four possible transition states (TS) for styrene insertion into the Ti−Me bond (two enantiofaces, *re* and *si*, two regiochemistries, 1,2 and 2,1, corresponding to primary and secondary styrene insertion, respectively). The configuration of the complex is always Δ. The obtained TSs are reported in Figure 6. This system allows to focus on the interaction between the monomer and the catalyst.

As indicated by the short distances reported in Figure 6, TSs 1,2-*si* and 2,1-*re* are characterized by steric clashes between the aromatic ring of the monomer and one of the ^{t}Bu groups of the catalyst. In addition, TS 2,1-*re* is also destabilized by additional steric clashes with the nearby C_6F_5 ring. These steric clashes destabilize both TSs (see the relatively high energy of these TSs in Figure 6) and, considering that

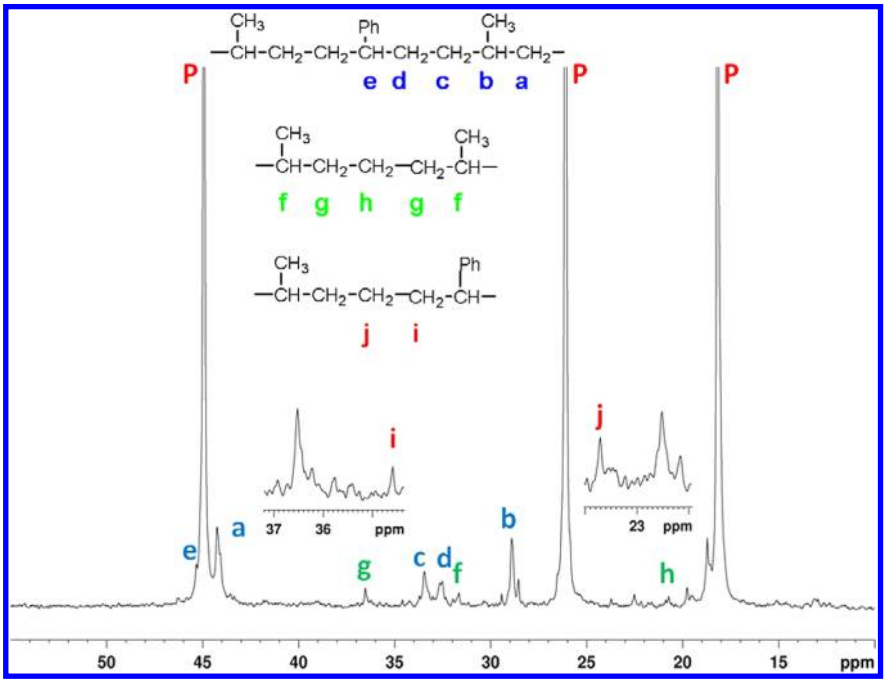

Figure 5. Aliphatic region of ^{13}C NMR spectrum (75 MHz, TCDE, 393 K) of the P(S−E/P) copolymer of run 3 of Table 3. The chemical shifts are in ppm downfield of HMDS.

dx.doi.org/10.1021/ma301631b | *Macromolecules* 2012, 45, 8588−8597

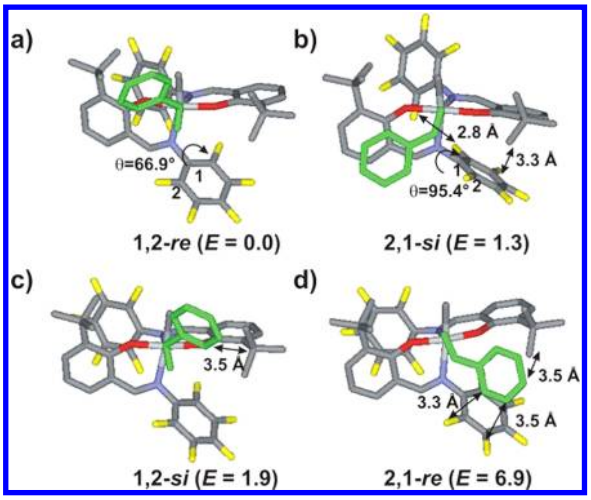

Figure 6. Transition state geometries for styrene insertion into the Ti−Me bond in case of a **ΔTi−FI** system. θ is defined as the Ti−N−C_1−C_2 torsional angle. For the sake of clarity, styrene is colored in green, and all the H atoms are omitted. Energies in kcal/mol.

these are steric clashes between the monomer and the ligand, they do not depend from the nature of the growing chain. For this reason, they will not be discussed any further.

This preliminary analysis allows focusing on the competition between the low energy 1,2-*re* and 2,1-*si* TSs for styrene insertion into a Ti−chain bond. Comparison of the these two TSs indicates that TS 1,2-*re* is favored by only 1.3 kcal/mol with respect to TS 2,1-*si*. Steric interactions between the monomer and the catalyst are absent in both the 1,2-*re* and 2,1-*si* TSs, see Figure 6. The slightly higher energy of TS 2,1-*si* is probably due to the less stable geometry that the catalyst assumes to minimize steric interactions between two ligands of the catalyst (see F−F distance of 2.8 Å and F−C distance of 3.3 Å in Figure 6b). In short, in qualitative agreement with the experiments, calculations indicate that in case of insertion into the Ti−Me bond of **Ti−FI,** styrene insertion should be scarcely regioselective. Further, considering that the short Me chain does not interact with the monomer, these calculations indicate that both 1,2- and 2,1-insertion of styrene are stereoselective, due to direct interaction between the monomer and the ligand, and that a Δ site selects the *re* and *si* enantiofaces of styrene in case of 1,2- and 2,1-insertion, respectively (by symmetry, a Λ site selects the *si* and *re* enantiofaces of styrene in case of 1,2- and 2,1-insertion, respectively).

To investigate the influence of the nature of the growing chain on the styrene insertion modes, we examined styrene insertion into the Ti−Et, Ti−^{i}Pr and Ti−^{i}Bu bonds for a Δ site of the **Ti−FI** system. Consistently with the above results, in all the cases calculations indicate a competition between 1,2-*re*-styrene and 2,1-*si*-styrene insertions. The relative energy and structure of these TSs are shown in Figure 7.

The energy differences reported in Figure 7 indicate that, different from insertion into a Ti−Me bond, 2,1-*si*-styrene insertion is favored. This difference is rather small in case of insertion into the Ti−Et bond, and it increases with increasing chain bulkiness. This trend can be explained by direct steric interaction between the monomer and the growing chain in the 1,2-*re*-TSs. This result is in rather good agreement with experiments, since insertion into the Ti−Et bond is substantially non regioselective, as experimentally found in the styrene-ethene-propene copolymerizations. Further, the preference for 2,1-insertion into a Ti−^{i}Pr bond is in qualitative agreement with the experimental evidence that in styrene−propene copolymerization insertion of the two comonomers occurs with the same regiochemistry.[6b,14f,26] Finally, the slightly higher preference for 2,1-insertion into a Ti−^{i}Bu bond relative to insertion into a Ti−^{i}Pr bond is in qualitative agreement with the experimental evidence of a higher preference for 2,1-styrene insertion into a Ti−1,2-styrene growing chain. In short, in agreement with the experiments, calculations indicate an inversion of

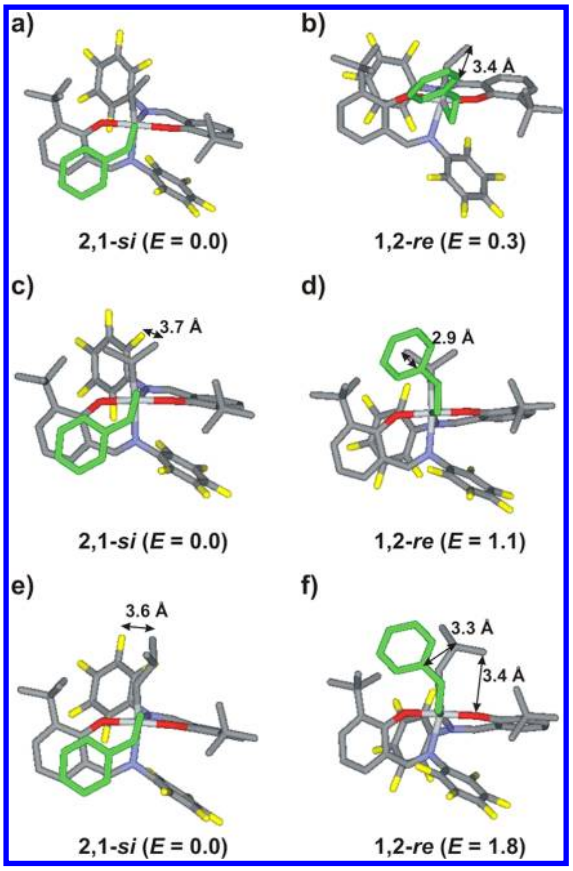

Figure 7. Transition states geometries for styrene insertion into the Ti−Et bond (a, b), the Ti−^{i}Pr bond (c, d) and the Ti−^{i}Bu bond (e, f) of a Δ site of **Ti−FI.** For the sake of clarity, styrene is colored in green, and all the H atoms are omitted. Energies in kcal/mol.

regioselectivity in styrene insertion, from 1,2, to nonregioselective, to 2,1, as the bulkiness of the growing chain increases from Me, to Et, to ^{i}Pr or ^{i}Bu. This consistency between calculations and experiments corroborates the whole chemical scenario proposed in this work.

We move now to styrene homopolymerization. To isolate effects, we first investigated the influence of the chirality of the growing chain on the chirality of the catalytic site for both a 2,1-*si*-ending styrene chain (modeled with a 1-phenylpropyl group), and a 1,2-*si*-ending styrene chain (modeled with a 2-phenylpropyl group). To this end, we located the TSs for ethene insertion on catalytic sites presenting both Δ (Figure 8, parts a and c) and Λ (Figure 8, parts b and d) configurations. Using ethene as the monomer removes the influence of the chiral coordination of styrene.

According to calculations, the TS for ethene insertion on a Δ-site is favored over the TS for insertion on a Λ-site both for primary (or 1,2) and secondary (or 2,1) *si*-ending styrene chains. This preference is higher in the case of a secondary chain, 3.6 kcal/mol, than for a primary growing chain, 1.4 kcal/mol. As indicated by the short distances in Figure 8, these preferences are mainly connected to steric repulsion involving the aromatic ring of the chain and the *ortho* substituent of the nearby phenoxy group as well as one of the C_6F_5 rings of the ligand. Thus, in the assumption of a fast Δ−Λ isomerization of the **Ti−FI** system, calculations indicate that both secondary and primary *si*-ending styrene growing chains should induce a Δ configuration at the catalytic site (by symmetry, the secondary and primary *re*-ending chains should induce a Λ configuration at the catalytic site).

Having clarified that both primary and secondary *si*-ending styrene chains induce a Δ configuration at the catalytic site, we examined 1,2-*re*- and 2,1-*si*-styrene insertion on both secondary and primary *si*-ending styrene chain a Δ **Ti-FI** catalytic site. The located TSs

dx.doi.org/10.1021/ma301631b | *Macromolecules* 2012, 45, 8588−8597

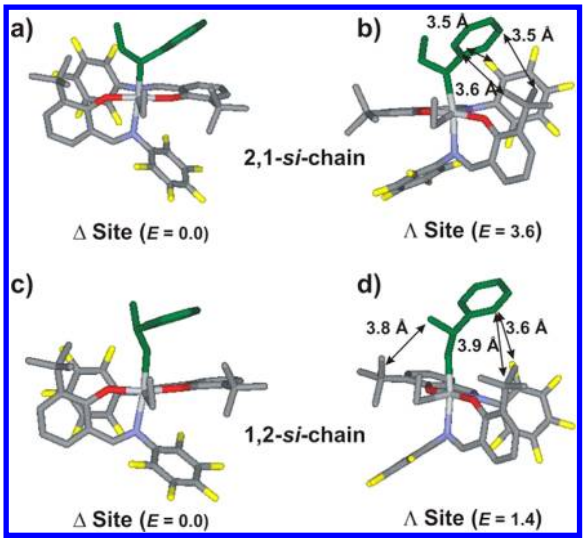

Figure 8. Transition states for ethene insertion into a Ti−2,1-*si*-styrene chain bond for Δ (a) and Λ (b) **TI-FI** sites, and into a Ti−1,2-*si*-styrene chain bond for Δ (c) and Λ (d) **Ti−FI** sites. For the sake of clarity, polymer chain is colored in green, and all the H atoms are omitted. Energies in kcal/mol.

geometries and the corresponding energies are sketched in Figure 9. As indicated previously, the high energy TSs for 2,1-*re*- and 1,2-*si*-styrene insertion were not considered.

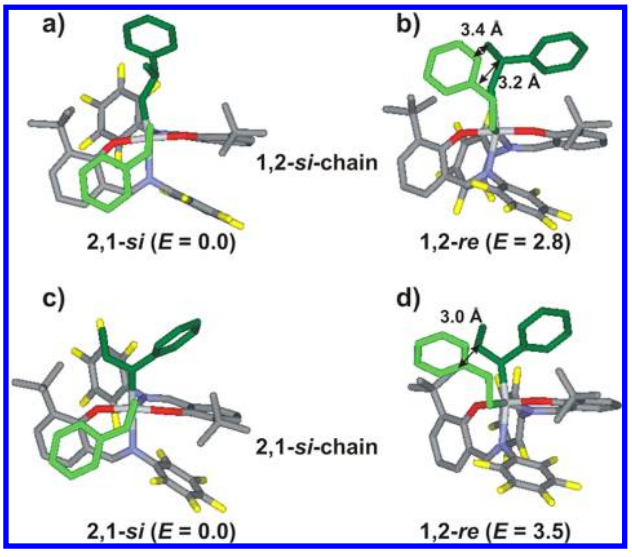

Figure 9. Transition states for styrene insertion into a Ti−1,2-*si*-styrene chain bond (a and b) and into a Ti−2,1-*si*-styrene chain bond (c and d) for a Δ **Ti−FI** site. For the sake of clarity, styrene is colored in green, and all the H atoms are omitted. Energies in kcal/mol.

According to calculations, in the case of a primary *si*-ending styrene growing chain 2,1-*si*-styrene insertion is favored by 2.8 kcal/mol over a 1,2-*re*-styrene insertion. This preference increases to 3.5 kcal/mol in case of styrene insertion on a secondary *si*-ending styrene chain. In short, 2,1-*si*-styrene insertion is preferred both for primary and secondary styrenic growing chains, indicating that the preferred regiochemistry of styrene insertion during homopolymerization is 2,1. This conclusion is in agreement with the experimental results described above. Consistently with the origin of regioselectivity in case of styrene insertion into a Ti−^{i}Pr or Ti−^{i}Bu bond, see Figure 7, steric interaction between the monomer and the chain favor 2,1-*si*-styrene both for primary and secondary styrenic growing chain, see Figure 9.

As for the stereoregularity of the resulting polystyrene, calculations indicate that a 2,1-*si*-ending chain induces a Δ-site that, in turn, favors insertion of another 2,1-*si*-styrene, thus generating a meso diad (by symmetry, it is clear that a 2,1-*re*-ending chain induces a Λ-site that, in turn, favors insertion of another 2,1-*re*-styrene). This sequence of event explains the experimental formation an isotactic polymer. According to this mechanism, the configuration of the catalytic site is kept until a stereomistake occurs. This is a sharp difference with respect to the mechanism of propene polymerization by the same catalysts (see Scheme 3). In fact, in propene polymerization a *si*-ending chain favors a Δ-site that, in turn, favors insertion of a 2,1-*re*-propene, thus generating a racemic diad. The so generated *re*-ending chain would induce an inversion of configuration at the catalytic cycle from Δ to Λ, which would in turn favor insertion of a *si*-propene. This sequence of events explains formation of a syndiotactic polymer. Incidentally, an extremely similar mechanism was proposed to explain the syndioselective polymerization of styrene promoted by mono-Cp Ti−catalysts.[28]

Considering a Δ-site/*si*-chain diastereoisomer of the catalyst, if a stereomistake occurs, which means that a 2,1-*re*-styrene molecule inserts, two scenarios are possible. In the first, inversion of complex configuration of the formed Δ-site/*re*-chain diastereoisomer to the more stable Λ-site/*re*-chain diastereoisomer is slow with respect to insertion of another styrene molecule. In this case, the Δ-site would favor insertion of a *si*-styrene generating a stable Δ-site/*si*-chain diastereoisomer. In term of microstructure, the resulting polymer would present the *rr* stereoerrors, typical of a polymer produced within an enantiomorphic site stereocontrolled mechanism. In the second case, inversion of complex configuration of the formed Δ-site/*re*-chain diastereoisomer to the more stable Λ-site/*re*-chain diastereoisomer is fast with respect to insertion of another styrene molecule. The so formed Λ-site would favor insertion of a *re*-styrene generating a stable Λ-site/*re*-chain geometry. In term of microstructure, the resulting polymer would present isolated *r* stereoerrors, typical of a polymer produced within a chain-end stereocontrolled mechanism. Since experiments indicate the presence of isolated *r* stereoerrors, we conclude that inversion of configuration of the complex after a stereomistake is faster than insertion of another styrene molecule.

To have a complete comprehension of the mechanisms of stereoselectivity operative with **Ti−FI** catalysts, a more detailed comparison between styrene and propene polymerization is mandatory. The main difference between the two systems is in the relationship between the configuration of the growing chain, the configuration of the catalytic site and the monomer enantioface. In case of a *si*-ending chain both the styrene and the propene chain would favor a Δ site. In both cases, the preferred configuration of the catalytic site minimizes steric interaction with the groups at the Cα of the secondary growing chain. In case of propene, the two groups are a methyl group and the remaining part of the growing chain, which is of course bulkier than the single methyl group. In this case a Δ-site is preferred since it places the bulkier growing chain in an open part of space, while the methyl group suffers steric interaction with the ligand. Conversely, in the case of styrene the phenyl group at the Cα atom is bulkier than the β-CH_2 group and the following atoms of the growing chain. Thus, a Δ-site is preferred, since it places the bulkier phenyl group in an open part of space, while the remaining of the growing chain suffers steric interaction with the ligand. Finally, for the Δ site, steric interaction between the monomer and the ligand favor the *si* monomer enantioface in the styrene polymerization whereas in the propene polymerization the *re* propene is favored (Scheme 3).

■ CONCLUSIONS

In this work, we reported a detailed experimental and theoretical study of the mechanism of isotactic styrene polymerization promoted by the C_6F_5-substituted bis-(phenoxyimine) titanium catalyst. The main results can be summarized as follows. As evidenced by the NMR analysis of

dx.doi.org/10.1021/ma301631b | *Macromolecules* 2012, 45, 8588−8597

Scheme 3

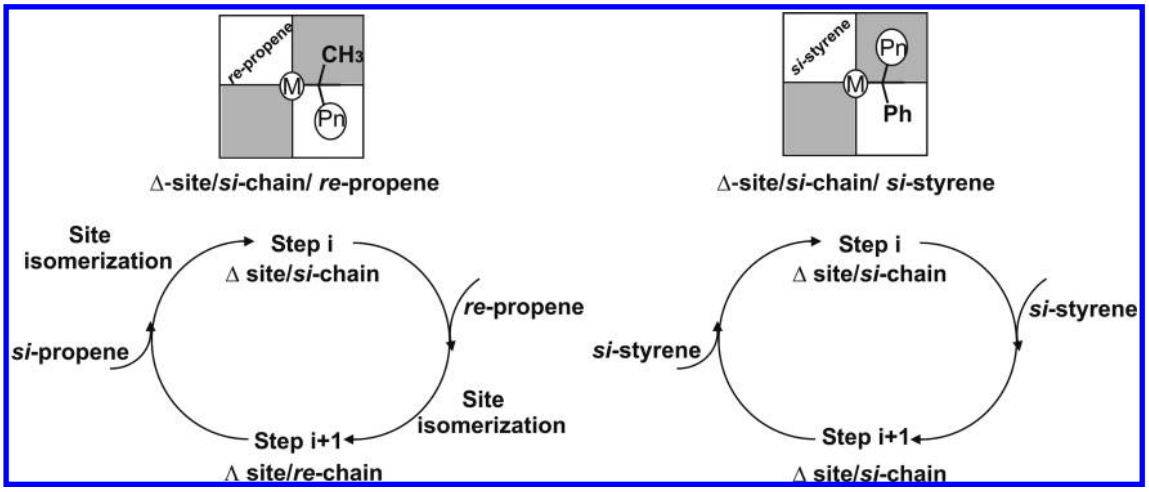

the styrene homopolymers and styrene copolymers with ethene and propene, regiochemistry of styrene insertion into a Ti–chain bond is essentially secondary. Further, the same kind of analysis indicated that the stereoerrors in the isotactic polystyrene chains are consistent with a chain-end stereocontrolled mechanism. DFT calculations rationalized these experimental findings indicating that primary styrene insertion is disfavored by steric interactions between the phenyl group of the monomer and the growing chain. The same interactions should be also responsible for the mechanism of stereocontrol. In this framework, the last inserted chiral monomeric unit of the growing chain forces one configuration of the catalytic site, which in turn selects one of the two enantiofaces of the secondary inserting styrene molecule.

Quadrants analysis indicated that the same configuration of the catalytic site is favored before and after styrene insertion, which explains the resulting isoselectivity. This is different from the case of propene insertion by the same catalysts. In fact, in this case opposite configurations of the catalyst are favored before and after propene insertion, which results in the inversion of configuration at the catalytic site at each insertion step, which explained the resulting syndioselectivity.

EXPERIMENTAL SECTION

General Remarks and Materials. All manipulations of air- and/or water sensitive compounds were carried out under a dry nitrogen atmosphere using a Braun Labmaster drybox or standard Schlenk line techniques.

All solvents, purchased from Carlo Erba, were purified and dried by refluxing over an appropriate agent before use them. Toluene and hexane were dried first over calcium chloride and then distilled over sodium under a nitrogen atmosphere.

Ethene and Propene were purchased from Societá Ossigeno Napoli and used without further purification. Styrene was stirred over CaH_2 and distilled under reduced pressure of nitrogen. Methylalumoxane (MAO), provided by Witco as a 30 wt % solution in toluene, was dried before the use by removing in vacuo the solvent.

Bis[*N*-(3-*tert*-butylsalicylidene)-2,3,4,5,6-pentafluoroanilinato]-titanium(IV) dichloride (**Ti-FI**) was synthesized according to the literature.[14c]

Styrene Polymerization. Polymerizations were carried out under reaction conditions reported in Table 1 according to a previous paper.[13] Under a nitrogen atmosphere, a magnetically stirred flask (50 mL) was sequentially charged with toluene, dried DMAO, and styrene. A toluene solution of precatalyst, dissolved in the minimum amount of solvent, was added to the flask.

After the prescribed time, the polymerization mixture was poured into acidified ethanol. Polymers were recovered by filtration and dried in a vacuum oven at 40 °C for 12 h.

Styrene–Propene Copolymerization. Copolymerizations were carried out in a 250 mL Pyrex reactor charged, under a nitrogen atmosphere, sequentially with styrene (100 mL) and DMAO. The mixture was magnetically stirred, and the glass flask was thermostated at 25 °C. The inert atmosphere was removed and replaced with the propene feed, and then 3 mL of a toluene solution of the **Ti–FI** were added.

The flask was fed with the gaseous monomer over the polymerization time.

The copolymers were coagulated by pouring the reaction mixture into acidified methanol, filtered, washed with further methanol and then with boiling acetone, and dried in vacuo.

Styrene–Ethene–Propene Copolymerization. The copolymers were obtained by bubbling (0.2 L/min) a gaseous mixture of ethane and propene prepared with an automatic gas blending device (MKS Instruments, Deutschland GmbH), at atmospheric pressure into a 250 mL Pyrex reactor provided with magnetic stirrer, containing toluene, styrene, DMAO, and catalyst (**Ti–FI**) at 25 °C. The copolymers were coagulated by pouring the reaction mixture into methanol acidified with HCl (aqueous, concentrated) and then filtered, washed with fresh methanol, and vacuum-dried. The gas mixtures of the monomers were analyzed by gas chromatography.

^{13}C NMR Analysis. The ^{13}C NMR spectra of polystyrene samples were recorded on an AV 400. Bruker operating at 100.6 MHz in the Fourier transform mode at 298 K . The copolymers were analyzed by a 300 MHz, operating at 75 MHz, at 383 K. The samples (30 mg) were dissolved in 0.5 mL of opportune deuterated solvent into a tube with 5 mm outer diameter. The polystyrene samples were dissolved in $CDCl_3$ whereas 1,1,2,2-tetrachloroethane-d_2 (TCDE) was used for the copolymers analyses and hexamethyldisiloxane (HMDS) was used as an internal chemical shift standard.

GPC Analysis. Molecular weights (M_n and M_w) and polydispersities (PDI) of the polymer samples were determined by high-temperature GPC using a Waters GPCV 2000 equipped with refractive index and viscometer detectors. The measurements were recorded at 120 °C using 1,2-dichlorobenzene as a solvent and Styragel columns (range 107 to 103) and standard polystyrene samples for calibration. Every value was the average of two independent measurements.

Computational Details. DFT calculations were performed with the Gaussian03 package,[29] using the BP86 functional,[30] the LANL2DZ/ECP and valence basis set for Ti[31] and the SVP basis set on all other atoms.[32] Minima were localized by full optimization of the starting structures, while transition states for monomer insertion were approached through a linear transit procedure starting from the monomer-coordinated intermediate and then located by a full

dx.doi.org/10.1021/ma301631b | *Macromolecules* 2012, 45, 8588–8597

transition state search. All structures were confirmed as minimum or transition state through frequency calculations.

■ ASSOCIATED CONTENT

Supporting Information

Additional experimental details regarding synthesis and characterization of polymers and copolymers, methine protons region of ^{1}H NMR spectrum of iPS obtained in run 4, Table1, transition state geometries and corresponding energies for styrene insertion into the Ti−Me, Ti−Et, Ti−^{i}Pr, and Ti−^{i}Bu, bonds for a Δ **Ti−FI** system, transition states for ethene insertion into a Ti−2,1-*si*-styrene chain bond for Δ and Λ **TI−FI** sites, and into a Ti−1,2-*si*-styrene chain bond for Δ and Λ **Ti−FI** sites, and transition states for styrene insertion into a Ti−1,2-*si*-styrene chain bond and into a Ti−2,1-*si*-styrene chain bond for a Δ **Ti−FI** site. This material is available free of charge via the Internet at http://pubs.acs.org/.

■ AUTHOR INFORMATION

Corresponding Author

*E-mail: (L.C.) lcaporaso@unisa.it; (T.F.) Terunori.Fujita@mitsui-chem.co.jp.

Notes

The authors declare no competing financial interest.

■ ACKNOWLEDGMENTS

We thank ENEA (www.enea.it) and the HPC team for support as for using the ENEA-GRID and the HPC facilities CRESCO (www.cresco.enea.it) Portici (Naples), Italy, for access to computational resources. Finally, we thank Dr. Patrizia Oliva (University of Salerno) for technical assistance for the NMR analyses.

■ REFERENCES

(1) (a) Möhring, P. C.; Conville, N. J. *J. Organomet. Chem.* **1994**, *479*, 1. (b) Guram, A. S.; Jordan, R. F. In *Comprehensive Organometallic Chemistry*, Second Edition, **1995**, *4*, 589. (c) Brintzinger, H. H.; Fischer, D.; Mülhaupt, R.; Rieger, B.; Waymouth, R. M. *Angew. Chem., Int. Ed. Engl.* **1995**, *34*, 1143. (d) Grubbs, R. H.; Coates, G. W. *Acc. Chem. Res.* **1996**, *29*, 85. (e) Bochmann, M. *J. Chem. Soc., Dalton Trans.* **1996**, 255. (f) Kaminsky, W. *Macromol. Chem. Phys.* **1996**, *197*, 3907. (g) Kaminsky, W. *J. Chem. Soc., Dalton Trans.* **1998**, 1413. (h) Alt, H. G.; Köppl, A. *Chem. Rev.* **2000**, *100*, 1205. (i) Coates, G. W. *Chem. Rev.* **2000**, *100*, 1223. (j) Resconi, L.; Cavallo, L.; Fait, A.; Piemontesi, F. *Chem. Rev.* **2000**, *100*, 1253. (k) Chen, E. Y. X.; Marks, T. J. *Chem. Rev.* **2000**, *100*, 1391. (l) Kaminsky, W. *Adv. Catal.* **2001**, *46*, 89. (m) Kaminsky, W. *J. Polym. Sci., Part A: Poly, Chem.* **2004**, *42*, 3911.

(2) (a) Mashima, K.; Nakayama, Y.; Nakamura, A. *Adv. Polym. Sci.* **1997**, *133*, 1. (b) McKnight, A. L.; Waymouth, R. M. *Chem. Rev.* **1998**, *98*, 2587. (c) Britovsek, G. J. P.; Gibson, V. C.; Wass, D. F. *Angew. Chem., Int. Ed.* **1999**, *38*, 428. (d) Ittel, S. D.; Johnson, L. K.; Brookhart, M. *Chem. Rev.* **2000**, *100*, 1169. (e) Coates, G. W. *J. Chem. Soc., Dalton Trans.* **2002**, 467. (f) Coates, G. W.; Hustad, P. D.; Reinartz, S. *Angew. Chem., Int. Ed.* **2002**, *41*, 2236. (g) Gibson, V. C.; Spitzmesser, S. K. *Chem. Rev.* **2003**, *103*, 283. (h) Qian, Y.; Huang, J.; Bala, M. D.; Lian, B.; Zhang, H.; Zhang, H. *Chem. Rev.* **2003**, *103*, 2633. (i) Park, S.; Han, Y.; Kim, S. K.; Lee, J.; Kim, H. K.; Do, Y. *J. Organomet. Chem.* **2004**, *689*, 4263. (j) Domski, G. J.; Rose, J. M.; Coates, G. W.; Bolig, A. D.; Brookhart, M. *Prog. Polym. Sci.* **2007**, *32*, 30.

(3) (a) Corradini, P.; Guerra, G.; Cavallo, L. *Acc. Chem. Res.* **2004**, *37*, 231. (b) Rodrigues, A.-S.; Kirillov, E.; Carpentier, J.-F. *Coord. Chem. Rev.* **2008**, *252*, 2115.

(4) (a) Suzuki, Y.; Kinoshita, S.; Shibahara, A.; Ishii, S.; Kawamura, K.; Inoue, Y.; Fujita, T. *Organometallics* **2010**, *29*, 2394. (b) Kinoshita, S.; Kawamura, K.; Fujita, T. *Chem. Asian J.* **2011**, *6*, 284.

(5) (a) Fujita, T.; Tohi, Y.; Mitani, M.; Matsui, S.; Saito, J.; Nitabaru, M.; Sugi, K.; Makio, H.; Tsutsui, T. *Eur. Pat. Appl.* 0 874 005, 199. (b) Makio, H.; Kashiwa, N.; Fujita, T. *Adv. Synth. Catal.* **2002**, *344*, 477. (c) Suzuki, Y.; Terao, H.; Fujita, T. *Bull. Chem. Soc. Jpn.* **2003**, *76*, 1493. (d) Mitani, M.; Saito, J.; Ishii, S.; Nakayama, Y.; Makio, H.; Matsukawa, N.; Matsui, S.; Mohri, J.; Furuyama, R.; Terao, H.; Bando, H.; Tanaka, H.; Fujita., T. *Chem. Rec.* **2004**, *4*, 137. (e) Fujita, T.; Makio, H. *Comprehensive Organometallic Chemistry III*; Elsevier: Oxford, U.K., 2007; p 691. (f) Matsugi, T.; Fujita, T. *Chem. Soc. Rev.* **2008**, *37*, 1264. (g) Makio, H.; Terao, H.; Iwashita, A.; Fujita, T. *Chem. Rev.* **2011**, *111*, 2363.

(6) (a) Mitani, M.; Nakano, T.; Fujita, T. *Chem.—Eur. J.* **2003**, *9*, 2396. (b) Sakuma, A.; Weiser, M.-S.; Fujita, T. *Polym. J.* **2007**, *39*, 193.

(7) Terao, T.; Ishii, S.; Saito, J.; Matsuura, S.; Mitani, M.; Nagai, N.; Tanaka, H.; Fujita, T. *Macromolecules* **2006**, *39*, 8584.

(8) Saito, J.; Tohi, Y.; Matsukawa, N.; Mitani, M.; Fujita, T. *Macromolecules* **2005**, *38*, 4955.

(9) Makio, H.; Ochiai, T.; Tanaka, H.; Fujita, T. *Adv. Synth. Catal.* **2010**, *352*, 1635.

(10) Terao, H.; Iwashita, A.; Ishii, S.; Tanaka, H.; Yoshida, Y.; Mitani, M.; Fujita, T. *Macromolecules* **2009**, *42*, 4359.

(11) Terao, H.; Ishii, S.; Mitani, M.; Tanaka, H.; Fujita, T. *J. Am. Chem. Soc.* **2008**, *130*, 17636.

(12) (a) Saito, J.; Onda, M.; Matsui, S.; Mitani, M.; Furuyama, R.; Tanaka, H.; Fujita, T. *Macromol. Rapid Commun.* **2002**, *23*, 1118. (b) Prasad, A. V.; Makio, H.; Saito, J.; Onda, M.; Fujita, T. *Chem. Lett.* **2004**, *33*, 250. (c) Mazzeo, M.; Strianese, M.; Lamberti, M.; Santoriello, I.; Pellecchia, C. *Macromolecules* **2006**, *39*, 7812.

(13) Michiue, K.; Onda, M.; Tanaka, H.; Makio, H.; Mitani, M.; Fujita, T. *Macromolecules* **2008**, *41*, 6289.

(14) (a) Saito, J.; Mitani, M.; Mohri, J.; Ishii, S.; Yoshida, Y.; Matsugi, T.; Matsui, S.; Kojoh, S.; Takagi, Y.; Inoue, Y.; Fujita, T.; Kashiwa, N. *Chem. Lett.* **2001**, 576. (b) Saito, J.; Mitani, M.; Mohri, J.; Yoshida, Y.; Matsui, S.; Ishii, S.; Kojoh, S.; Kashiwa, N.; Fujita, T. *Angew. Chem., Int. Ed.* **2001**, *40*, 2918. (c) Mitani, M.; Mohri, J.; Yoshida, Y.; Saito, J.; Ishii, S.; Tsuru, K.; Matsui, S.; Furuyama, R.; Nakano, T.; Tanaka, H.; Kojoh, S.; Matsugi, T.; Kashiwa, N.; Fujita, T. *J. Am. Chem. Soc.* **2002**, *124*, 3327. (d) Mitani, M.; Furuyama, R.; Mohri, J.; Saito, J.; Ishii, S.; Terao, H.; Kashiwa, N.; Fujita, T. *J. Am. Chem. Soc.* **2002**, *124*, 7888. (e) Mitani, M.; Mohri, J.; Furuyama, R.; Ishii, S.; Fujita, T. *Chem. Lett.* **2003**, 238. (f) Mitani, M.; Furuyama, R.; Mohri, J.; Saito, J.; Ishii, S.; Terao, H.; Nakano, T.; Tanaka, H.; Fujita, T. *J. Am. Chem. Soc.* **2003**, *125*, 4293.

(15) Nakayama, Y.; Saito, J.; Bando, H.; Fujita, T. *Chem. Eur. J.* **2006**, *12*, 7546.

(16) (a) Arai, T.; Ohtsu, T.; Suzuki, S. *Polym. Prepr* **1998**, *39*, 220. (b) Arai, T.; Ohtsu, T.; Suzuki, S. *Macromol. Rapid Commun.* **1998**, *19*, 327. (c) Arai, T.; Suzuki, S.; Ohtsu, T. *Olefin Polymerization*; ACS Symposium Series 749; American Chemical Society: Washington, DC, 2000, 66. (d) Caporaso, L.; Izzo, L.; Sisti, I.; Oliva, L. *Macromolecules* **2002**, *35*, 4866. (e) Izzo, L.; Napoli, M.; Oliva, L. *Macromolecules* **2003**, *36*, 9340. (f) Capacchione, C.; Proto, A.; Ebeling, H.; Mülhaupt, R.; Möller, K.; Spaniol, T. P.; Okuda, J. *J. Am. Chem. Soc.* **2003**, *125*, 4964. (g) Capacchione, C.; Manivannan, R.; Barone, M.; Beckerle, K.; Centore, R.; Oliva, L.; Proto, A.; Tuzi, A.; Spaniol, T. P.; Okuda, J. *Organometallics* **2005**, *24*, 2971. (h) Beckerle, K.; Capacchione, C.; Ebeling, H.; Manivannan, R.; Mülhaupt, R.; Proto, A.; Spaniol, T. P.; Okuda, J. *J. Organomet. Chem.* **2004**, *689*, 4636.

(17) (a) Zambelli, A.; Oliva, L.; Pellecchia, C. *Macromolecules* **1989**, *22*, 2129. (b) Grassi, A.; Zambelli, A.; Laschi, F. *Organometallics* **1996**, *15*, 480. (c) Grassi, A.; Saccheo, S.; Zambelli, A.; Laschi, F. *Macromolecules* **1998**, *31*, 5588.

(18) (a) Longo, P.; Grassi, A.; Oliva, L.; Ammendola, P. *Makromol. Chem.* **1990**, *191*, 237. (b) Oliva, L.; Caporaso, L.; Pellecchia, C.; Zambelli, A. *Macromolecules* **1995**, *28*, 4665. (c) Myagmarsuren, G.; Tkach, V. S.; Shmidt, F. K.; Mohamad, M.; Suslov, D. S. *J. Mol. Catal.*

2005, *235*, 154. (d) Resconi, L.; Fait, A.; Piemontesi, F.; Colonnesi, M.; Rychlicki, H.; Ziegler, R.; Resconi, L. *Macromolecules* **1995**, *28*, 6667. (e) Caporaso, L.; De Rosa, C.; Talarico, G. *J. Polym. Sci., Polym. Chem* **2010**, *48*, 699.
(19) Ammendola, P.; Tancredi, T.; Zambelli, A. *Macromolecules* **1986**, *19*, 307.
(20) Randall, J. C. *J. Polym. Sci., Polym. Phys. Ed.* **1975**, *13*, 889.
(21) Sato, H., Tanaka, Y. In *NMR and Macromolecules*; Randall, J. C., Ed.; ACS Symposium Series 247; American Chemical Society: Washington, DC, 1984; p 181.
(22) (a) Annunziata, L.; Rodrigues, A. S.; Kirillov, E.; Sarazin, Y.; Okuda, J.; Perrin, L.; Maron, L.; Carpentier, J.-F. *Macromolecules* **2011**, *44*, 3312. (b) Feil, F.; Harder, S. *Macromolecules* **2003**, *36*, 3446.
(23) We performed the styrene propene copolymerizations under the same reaction conditions reported in Table 2 with the corresponding non fluorinated system activated with DMAO and no copolymers we obtained.
(24) (a) Caporaso, L.; Izzo, L.; Oliva, L. *Macromolecules* **1999**, *32*, 7329. (b) Oliva, L.; Guerra, G.; Caporaso, L.; Izzo, L.; Resconi, L. US Patent 6,617,410. Montell Technology Company BV: Netherlands, 2003.
(25) (a) Caporaso, L.; Izzo, L.; Zappile, S.; Oliva, L. *Macromolecules* **2000**, *33*, 7275. (b) Caporaso, L.; Iudici, N.; Oliva, L. *Macromolecules* **2005**, *38*, 4894. (c) Caporaso, L.; Iudici, N.; Oliva, L. *Macromol. Symp.* **2006**, *234*, 42. (d) Caporaso, L.; Oliva, L. *J. Polym. Sci., Polym. Chem.* **2006**, *44*, 7008.
(26) (a) Makio, H.; Fujita, T. *Bull. Chem. Soc. Jpn.* **2005**, *78*, 52. (b) Tian, J.; Hustad, P. D.; Coates, G. W. *J. Am. Chem. Soc.* **2001**, *123*, 5134. (c) Furuyama, R.; Saito, J.; Ishii, S.; Mitani, M.; Matsui, S.; Tohi, Y.; Makio, H.; Matsukawa, N.; Tanaka, H.; Fujita, T. *J. Mol.Catal. A* **2003**, *200*, 31.
(27) (a) Milano, G.; Cavallo, L.; Guerra, G. *J. Am. Chem. Soc.* **2002**, *124*, 13368. (b) Talarico, G.; Busico, V.; Cavallo, L. *J. Am. Chem. Soc.* **2003**, *125*, 7172. (c) Lamberti, M.; Pappalardo, D.; Zambelli, A.; Pellecchia, C. *Macromolecules* **2002**, *35*, 658. (d) Hustad, P. D.; Tian, J.; Coates, G. W. *J. Am. Chem. Soc.* **2002**, *124*, 3614.
(28) (a) Ishihara, N.; Seimiya, T.; Kuramoto, M.; Uoi, M. *Macromolecules* **1986**, *19*, 2464. (b) Minieri, G.; Corradini, P.; Zambelli, A.; Guerra, G.; Cavallo, L. *Macromolecules* **2001**, *34*, 2459. (c) Minieri, G.; Corradini, P.; Guerra, G.; Zambelli, A.; Cavallo, L. *Macromolecules* **2001**, *34*, 5379.
(29) Frisch, J.; Trucks, G. W.; Schlegel, H. B.; Scuseria, G. E.; Robb, M. A.; Cheeseman, J. R.; Montgomery, J. A., Jr.; Vreven, T.; Kudin, K. N.; Burant, J. C.; Millam, J. M.; Iyengar, S. S.; Tomasi, J.; Barone, V.; Mennucci, B.; Cossi, M.; Scalmani, G.; Rega, N.; Petersson, G. A.; Nakatsuji, H.; Hada, M.; Ehara, M.; Toyota, K.; Fukuda, R.; Hasegawa, J.; Ishida, M.; Nakajima, T.; Honda, Y.; Kitao, O.; Nakai, H.; Klene, M.; Li, X.; Knox, J. E.; Hratchian, H. P.; Cross, J. B.; Bakken, V.; Adamo, C.; Jaramillo, J.; Gomperts, R.; Stratmann, R. E.; Yazyev, O.; Austin, V.; Cammi, R.; Pomelli, C.; Ochterski, J. W.; Ayala, P. Y.; Morokuma, K.; Voth, G. A.; Salvador, P.; Dannenberg, J. J.; Zakrzewski, V. G.; Dapprich, S.; Daniels, A. D.; Strain, M. C.; Farkas, O.; Malick, D. K.; Rabuck, A. D.; Raghavachari, K.; Foresman, J. B.; Ortiz, J. V.; Cui, Q.; Baboul, A. G..; Clifford, S.; Cioslowski, J.; Stefanov, B. B.; Liu, G.; Liashenko, A.; Piskorz, P.; Komaromi, I.; Martin, R. L.; Fox, D. J.; Keith, T.; Al-Laham, M. A.; Peng, C. Y.; Nanayakkara, A.; Challacombe, M.; Gill, P. M. W.; Johnson, B.; Chen, W.; Wong, M. W.; Gonzalez, C.; Pople, J. A. Gaussian 03, Revision C.02; Gaussian, Inc.: Wallingford CT, 2004.
(30) (a) Becke, A. D. *Phys. Rev. A* **1988**, *38*, 3098. (b) Perdew, J. P. *Phys. Rev. B* **1986**, *34*, 7406. (c) Perdew, J. P. *Phys. Rev. B* **1986**, *33*, 8822.
(31) (a) Dunning, T. H., Jr.; Hay, P. J. In *Modern Theoretical Chemistry*; Schaefer, H. F., III, Ed.; Plenum: New York, 1976, Vol. 3 (b) Hay, P. J.; Wadt, W. R. *J. Chem. Phys.* **1985**, *82*, 270.
(32) (a) Schaefer, A.; Horn, H.; Ahlrichs, R. *J. Chem. Phys.* **1992**, *97*, 2571. (b) Schaefer, A.; Huber, C.; Ahlrichs, R. *J. Chem. Phys.* **1994**, *100*, 5829.